NASA Contractor Report 187516
ICASE Report No. 91–14

ICASE

NUMERICAL RECOVERY OF MATERIAL PARAMETERS IN EULER-BERNOULLI BEAM MODELS

R. C. Smith
K. L. Bowers
C. R. Vogel

Contract No. NAS1–18605
February 1991

Institute for Computer Applications in Science and Engineering
NASA Langley Research Center
Hampton, Virginia 23665–5225

Operated by the Universities Space Research Association

National Aeronautics and Space Administration

Langley Research Center
Hampton, Virginia 23665-5225

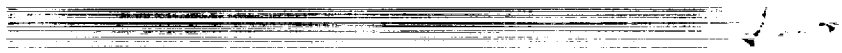

NUMERICAL RECOVERY OF MATERIAL PARAMETERS IN EULER-BERNOULLI BEAM MODELS

R.C. Smith[1]
Institute for Computer Applications in Science and Engineering
NASA Langley Research Center
Hampton, VA 23665

K.L. Bowers and C.R. Vogel
Department of Mathematical Sciences
Montana State University
Bozeman, MT 59717

ABSTRACT

A fully Sinc-Galerkin method for recovering the spatially varying stiffness parameter in fourth-order time-dependent problems with fixed and cantilever boundary conditions is presented. The forward problems are discretized with a sinc basis in both the spatial and temporal domains. This yields an approximate solution which converges exponentially and is valid on the infinite time interval. When the forward methods are applied to parameter recovery problems, the resulting inverse problems are ill-posed. Tikhonov regularization is applied and the resulting minimization problems are solved via a quasi-Newton/trust region algorithm. The L-curve method is used to determine an appropriate value of the regularization parameter. Numerical results which highlight the method are given for problems with both fixed and cantilever boundary conditions.

[1]This research was supported by the National Aeronautics and Space Administration under NASA Contract No. NAS1-18605 while the author was in residence at the Institute for Computer Applications in Science and Engineering (ICASE), NASA Langley Research Center, Hampton, VA 23665.

1 Introduction

In this paper, a fully Sinc-Galerkin method is introduced for the numerical recovery of material parameters in fourth-order time-dependent problems. To illustrate the method, consider the problem of estimating the spatially varying parameter $EI(x)$ in the state equations

$$\begin{aligned} \mathcal{L}(EI)u \equiv \frac{\partial^2 u}{\partial t^2} + \frac{\partial^2}{\partial x^2}\left(EI(x)\frac{\partial^2 u}{\partial x^2}\right) = f(x,t), \quad 0 < x < 1 \quad t > 0 \\ u(0,t) = u(1,t) = 0, \quad t > 0 \\ \frac{\partial u}{\partial x}(0,t) = \frac{\partial u}{\partial x}(1,t) = 0, \quad t > 0 \\ u(x,0) = \frac{\partial u}{\partial t}(x,0) = 0, \quad 0 \le x \le 1 \end{aligned} \tag{1.1}$$

and

$$\begin{aligned} \mathcal{L}(EI)u = f(x,t), \quad 0 < x < 1, \ t > 0 \\ u(0,t) = \overline{\alpha}(t), \ \left(EI\frac{\partial^2 u}{\partial x^2}\right)(1,t) = \overline{\gamma}(t), \quad t > 0 \\ \frac{\partial u}{\partial x}(0,t) = \overline{\beta}(t), \quad \frac{\partial}{\partial x}\left(EI\frac{\partial^2 u}{\partial x^2}\right)(1,t) = \overline{\delta}(t), \quad t > 0 \\ u(x,0) = \frac{\partial u}{\partial t}(x,0) = 0, \quad 0 \le x \le 1 \end{aligned} \tag{1.2}$$

given measurements of the data at the points $\{(x_p, t_q)\}_{p=1,\cdots,n_p}^{q=1,\cdots,n_q}$ in $(0,1)\times I\!R^+$. These formulations are generalizations of the equations which arise when using the Euler-Bernoulli theory to model beams with flexural rigidity $EI(x)$ and fixed and cantilever ends, respectively. For ease of presentation throughout the paper, the boundary conditions in (1.1) and (1.2) will be referred to as fixed and cantilever conditions with the general $\overline{\gamma}(t)$ and $\overline{\delta}(t)$ included to allow for boundary controllers.

Since $EI(x)$ denotes the flexural stiffness, it is physically reasonable to assume that EI is continuous on $[0,1]$ and to let the admissible parameter set Q be defined by

$$Q = \{EI \in H^2(0,1) : EI(x) \ge EI_0 > 0\}$$

(see [9]). With this definition, the existence of a unique solution u to the forward problem can be obtained on any fixed time interval $[0,\tau], \tau > 0$, for f sufficiently smooth.

In order to apply the results from classical operator theory, the inverse problems corresponding to (1.1) and (1.2) can be written as operator equations of the form $\mathcal{K}(EI) = d$ where $\mathcal{K}$ is compact. The procedure for problems with fixed boundary conditions is outlined below with the formulation for problems with cantilever boundary conditions following similarly. Further theory for this latter case can be found in [1].

In formulating the operator equation corresponding to (1.1), it is easiest to first consider the spatial problem

$$\begin{aligned} &(EI(x)u'')'' - q(x)u = f(x), \quad 0 < x < 1 \\ &u(0) = u(1) = u'(0) = u'(1) = 0 \end{aligned} \tag{1.3}$$

where $EI(x)$ and $q(x)$ are both strictly positive on $[0,1]$. From the theory of [10] as noted in [20], there exists a Green's function for (1.3) which will be denoted by $G(x,s,EI(s))$ to emphasize its dependence on EI. It follows that G and $\frac{\partial G}{\partial EI}$ are continuous on [0,1] and that the state solution u is given by

$$u(x) = \int_0^1 G(x,s,EI(s))f(s)ds.$$

(see [20], pages 205-206).

These one-dimensional results can then be extended to the time-dependent problem (1.1) via a separation of variables. The substitution of $u(x,t) = X(x)T(t)$ into the homogeneous problem corresponding to (1.1) yields

$$T''(t) + \lambda T(t) = 0$$

and the eigenvalue problem

$$\begin{aligned} &(EI(x)X''(x))'' - \lambda X(x) = 0, \qquad 0 < x < 1 \\ &X(0) = X(1) = X'(0) = X'(1) = 0 \end{aligned}$$

where $\lambda > 0$. From arguments similar to those in [5] and [20], it follows that since $EI(x) > 0$ on [0,1], the state solution to (1.1) can be represented by

$$u(x,t) = \int_0^1 \mathcal{G}(x,t,s,EI(s))ds.$$

The function $\mathcal{G}$ depends on a Green's function as well as the expansions of $T(t)$ and the forcing function f. Hence $\mathcal{G}$ is continuous with respect to EI and $\frac{\partial \mathcal{G}}{\partial EI}$ is bounded on $(0,1) \times (0,\tau]$ for f sufficiently smooth.

The inverse problem can then be written as the operator equation

$$\mathcal{K}(EI) = d \tag{1.4}$$

where d denotes the data. The nonlinear operator $\mathcal{K} : H^2(0,1) \to L^2((0,1)\times(0,\tau])$ is defined by

$$\mathcal{K}(EI) = \mathcal{C} \int_0^1 \mathcal{G}(\cdot,\cdot,s,EI(s))ds \tag{1.5}$$

where the observation operator $\mathcal{C}$ maps the state solution into the infinite dimensional observation space by

$$\mathcal{C}\psi(x,t) = \{\psi(x,t)\} \; ; \tag{1.6}$$

that is, $\mathcal{C}$ samples functions continuously throughout $(0,1) \times (0,\tau]$. Note that the choice $L^2((0,1) \times (0,\tau])$ for observation space is physically reasonable.

To show that $\mathcal{K}$ is compact, it is first shown that it is weakly continuous; that is, $EI_n \xrightarrow{w} EI$ in $H^2(0,1)$ implies that $\mathcal{K}(EI_n) \to \mathcal{K}(EI)$ in the L^2 norm. For every (x,t) in $(0,1) \times (0,\tau]$ it follows that

$$\begin{aligned}
&\left| \mathcal{C} \int_0^1 \mathcal{G}(x,t,s,EI_n(s))ds - \mathcal{C} \int_0^1 \mathcal{G}(x,t,s,EI(s))ds \right| \\
&\quad \leq \int_0^1 \left| \frac{\partial \mathcal{G}}{\partial EI}(x,t,s,\xi_n(s)) \right| \, |EI_n(s) - EI(s)|ds \\
&\quad \leq \mathcal{M} \int_0^1 |EI_n(s) - EI(s)|ds \\
&\quad \leq \mathcal{M} \max_{s\in[0,1]} |EI_n(s) - EI(s)|
\end{aligned}$$

with the last inequality resulting from the continuity of EI on $[0,1]$. Since weak convergence in $H^2(0,1)$ implies uniform convergence, it follows that $\mathcal{K}(EI_n)$ converges uniformly to $\mathcal{K}(EI)$. The weak continuity of $\mathcal{K}$ results from the fact that the uniform norm is stronger than the L^2 norm. Hence the operator $\mathcal{K}$ as defined in (1.5) is compact since weak continuity implies compactness.

Although the procedure just outlined was for the problem (1.1), similar results can be obtained for (1.2) once a Green's function has been found which satisfies the boundary conditions. Further theory on problems of this type can be found in [1] and [10].

Consider now the well-posedness of (1.4). First, since $\mathcal{G}$ is continuous, the range of the operator $\mathcal{K}$ lies in $C((0,1) \times (0,\tau])$ for any $EI \in Q$. Hence there exist elements $d \in L^2((0,1) \times (0,\tau])$ for which (1.4) has no solution. Furthermore, since $\mathcal{K}$ is a compact operator with an infinite dimensional range, it follows that the Moore-Penrose generalized inverse $\mathcal{K}^\dagger$ is discontinuous. This in turn indicates that small perturbations in the data d may give rise to arbitrarily large perturbations in the solution $EI \in Q$. Consequently, some sort of regularization (i.e., stabilization) is required to obtain an accurate approximation for EI.

The regularization technique that is used is Tikhonov regularization [24] , and the problem (1.4) is replaced by the minimization problem

$$\min_{EI \in Q} \mathcal{T}_\alpha(EI) \tag{1.7}$$

where

$$\mathcal{T}_\alpha(EI) \equiv \frac{1}{2}\{\|\mathcal{K}(EI) - d\|^2 + \alpha \mathcal{J}(EI)\}.$$

Here $\alpha > 0$ is a regularization parameter which controls the tradeoff between goodness of fit to the data and stability. The penalty functional $\mathcal{J}(EI)$ provides stability and allows the inclusion of *a priori* information about the true parameter EI. Since EI is assumed to be "smooth" in the sense that $EI \in H^2(0,1)$, the penalty functional is taken to be the norm

$$\mathcal{J}(EI) = \|EI\|_Q^2 \equiv \int_0^1 [EI''(x)]^2 dx + \varepsilon \int_0^1 [EI(x)]^2 dx. \tag{1.8}$$

with ε of order 10^{-6}. The reasons for including the second term and forcing $\mathcal{J}$ to be strictly positive will be discussed in the fourth section of the paper. By using arguments similar to those in [7] and [16] and assuming that $\mathcal{K}(EI)$ is one to one, it can be shown that with this definition for $\mathcal{J}(EI)$, the solutions EI_α to (1.7) converge as the regularization parameter $\alpha \to 0$ and as the perturbations in the data and operator tend to zero.

Due to the infinite dimensionality of Q and that of the state space, the problem (1.7) is an infinite dimensional minimization problem. In order to develop a practical numerical scheme, the problem must be replaced by a sequence of finite dimensional problems; that is, one must approximate the operator $\mathcal{K}$ and minimize the functional $\mathcal{T}_\alpha$ over a finite dimensional admissible subspace of Q.

The evaluation of $\mathcal{K}(EI)$ requires the solution of the partial differential equations (PDE's) (1.1) or (1.2). Similar PDE's must be solved to obtain the components of the derivative $\mathcal{K}'(EI)$. The construction of an approximate solution to these forward problems commonly begins with a Galerkin discretization of the spatial variable with time-dependent coefficients. This yields a system of ordinary differential equations which is solved via differencing techniques. Due to stability constraints on the discrete evolution operator, low order methods with small time steps are often required to obtain accurate approximations. Moreover, this time-stepping must be repeated at each step in the minimization of (1.7). A final difficulty lies in the need to interpolate at data points which do not coincide with the nodes of the ODE solver.

In contrast, the method of this work implements a Galerkin scheme in time as well as space. This method thus bypasses many of the difficulties associated with time-stepping methods in the context of inverse problems. Corresponding results for the heat equation can be found in [12] and [19].

The fully Sinc-Galerkin method in space and time has many salient features due both to the properties of the basis functions and the manner in which the problem is discretized. Perhaps the most distinctive feature of the method is the resulting exponential convergence rate when solving the corresponding forward problems. Furthermore, the judicious choice of a conformal map provides approximate solutions which are valid on the infinite time interval rather than only on a truncated time domain. Finally, the discrete system requires no numerical integrations to fill either the coefficient matrices or the right-hand side matrix. All three features prove to be advantageous when solving the forward problems and hence the inverse problem.

The foundations of the Sinc-Galerkin method are described in Section 2. The fundamental quadrature rules are given, and the exponential convergence rate of this method is stated. A thorough review of sinc function properties can be found in [22] and [23].

In the third section, the Sinc-Galerkin systems for the forward problems are constructed and implementation details are discussed. The section includes the outline of a very robust and accurate algorithm for solving the resulting matrix systems.

Section 4 includes the finite dimensional minimization problem with the discussion cen-

tering around the construction of the various components of the Tikhonov functional. The resulting unconstrained optimization problems are solved via a quasi-Newton/trust region algorithm as described in [2] and [8].

Numerical results are presented in Section 5. Of the many examples tested, those discussed in this section best exhibit the features necessary for the practical implementation of the method. A brief discussion of the L-curve technique [6] for determining the regularization parameter α is given at the beginning of the section, and the applicability of this technique in conjunction with the Sinc-Galerkin method is demonstrated by the numerical results. Finally, results are included both from data sets with white noise and from data sets to which no noise was added. As shown in these examples, the Sinc-Galerkin method works equally well in both cases.

2 Sinc Function Properties

For the Sinc-Galerkin method, the basis functions are derived from the Whittaker cardinal (sinc) function

$$sinc(x) \equiv \frac{\sin(\pi x)}{\pi x}, \quad -\infty < x < \infty \tag{2.1}$$

and it translates

$$S(k,h)(x) \equiv sinc\left(\frac{x-kh}{h}\right), \quad h > 0.$$

For $h^* = \frac{\pi}{4}$, three adjacent members of this sinc family $(S(k,h^*)(x), k = -1,0,1)$ are shown in Figure 1.

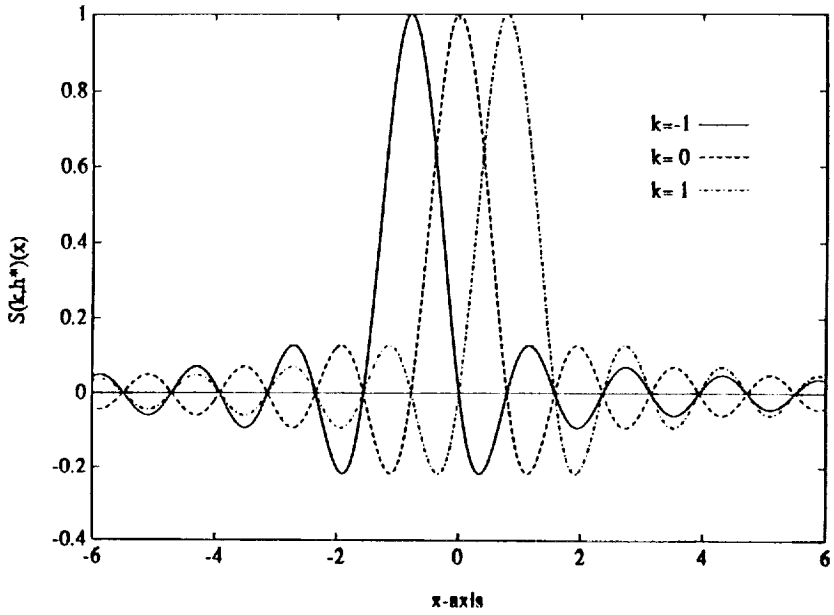

Figure 1. Three Adjacent Members $\left(S(k,h^*)(x), k=-1,0,1, h^*=\frac{\pi}{4}\right)$ of the Translated Sinc Family.

To construct basis functions on the intervals (0,1) and $(0,\infty)$, respectively consider the conformal maps

$$\phi(z) = ln\left(\frac{z}{1-z}\right) \tag{2.2}$$

and

$$\Upsilon(w) = ln(w). \tag{2.3}$$

The map ϕ carries the eye-shaped region

$$D_E = \left\{z = x+iy : \left|arg\left(\frac{z}{1-z}\right)\right| < d \leq \frac{\pi}{2}\right\} \tag{2.4}$$

onto the infinite strip

$$D_S = \{\xi = \zeta + i\eta : |\eta| < d \leq \frac{\pi}{2}\}. \tag{2.5}$$

Similarly, the map Υ carries the infinite wedge

$$D_W = \{w = t+is : |arg(w)| < d \leq \frac{\pi}{2}\} \tag{2.6}$$

onto the strip D_S. These regions are depicted in Figure 2.

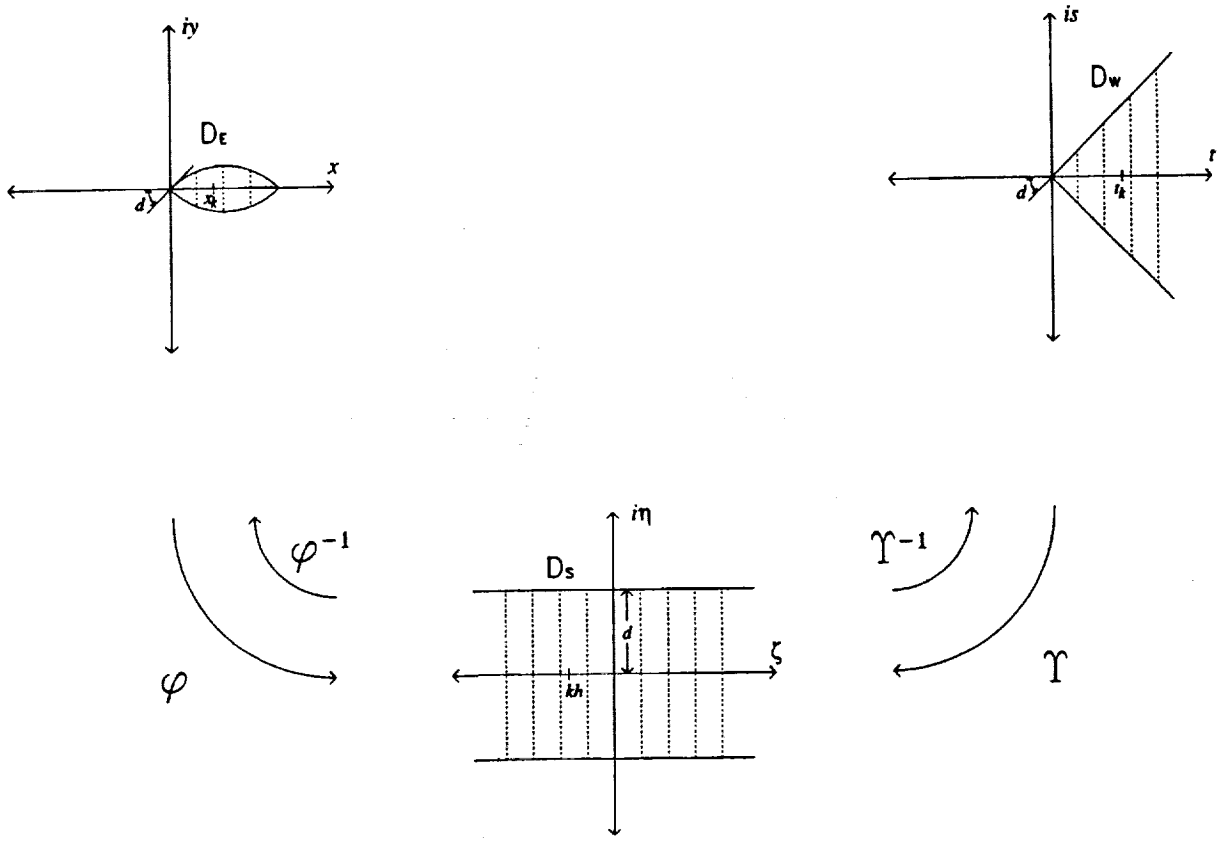

Figure 2. The Domains D_S, D_E, and D_W.

The sinc gridpoints $z_k \in (0,1)$ in D_E will be denoted x_k since they are real. Similarly, the gridpoints $w_k \in (0,\infty)$ in D_W will be denoted t_k. Both are inverse images of the equispaced grid in D_S; that is,

$$x_k = \phi^{-1}(kh) = \frac{e^{kh}}{1+e^{kh}} \tag{2.7}$$

and

$$t_k = \Upsilon^{-1}(kh) = e^{kh}. \tag{2.8}$$

To simplify notation throughout the remainder of this section, the pairs ϕ, D_E and Υ, D_W are referred to generically as χ, D. It is understood that the subsequent definition, theorems, and identities hold in either setting. Furthermore, the inverse of χ is denoted by ψ.

The important class of functions for sinc interpolation and quadrature is denoted $B(D)$ and defined next.

Definition 2.1. *Let $B(D)$ be the class of functions F which are analytic in D, satisfy*

$$\int_{\psi(t+L)} |F(z)dz| \to 0, \quad t \to \pm\infty$$

where $L = \{is : |s| < d < \frac{\pi}{2}\}$, and on the boundary of D (denoted ∂D) satisfy

$$N(F) \equiv \int_{\partial D} |F(z)dz| < \infty.$$

The following theorem for functions in $B(D)$ is found in [21].

Theorem 2.1. *Let Γ be $(0,1)$ or $(0,\infty)$ when $\chi = \phi$ or Υ, respectively. If $F \in B(D)$ and $z_j = \psi(jh) = \chi^{-1}(jh)$, $j = 0, \pm 1, \pm 2, \cdots$, then for $h > 0$ sufficiently small*

$$\left| \int_\Gamma F(z)dz - h \sum_{j=-\infty}^{\infty} \frac{F(z_j)}{\chi'(z_j)} \right| \leq K_1 e^{-2\pi d/h}. \tag{2.9}$$

Theorem 2.1 illustrates the exponential convergence rate which is a trademark of the sinc methods. There is a common occasion when it is possible to evaluate the infinite series appearing in (2.9), namely when integrating against $S(k,h) \circ \chi$. In general, however, the series must be truncated. With additional hypotheses, it is proven in [11] and [22] that the truncation need not be at the expense of the exponential convergence.

Theorem 2.2. *Assume $F \in B(D)$ and that there exist positive constants K, α, and β such that*

$$\left| \frac{F(\tau)}{\chi'(\tau)} \right| \leq K \begin{cases} e^{-\alpha|\chi(\tau)|}, & \tau \in \psi((-\infty, 0)) \\ e^{-\beta|\chi(\tau)|}, & \tau \in \psi([0,\infty)). \end{cases} \tag{2.10}$$

Then for h sufficiently small

$$\left| \int_\Gamma F(z)dz - h \sum_{j=-M}^{N} \frac{F(z_j)}{\chi'(z_j)} \right| \leq K_1 e^{-2\pi d/h} + \frac{K}{\alpha} e^{-\alpha M h} + \frac{K}{\beta} e^{-\beta N h}. \tag{2.11}$$

Theorems 2.1 and 2.2 are used to establish a uniform error bound when constructing an approximate solution to the forward fourth-order time-dependent problems. The application of these quadrature theorems is facilitated by the identities

$$\delta_{pi}^{(0)} \equiv [S(p,h) \circ \chi(z)]\Big|_{z=z_i} = \begin{cases} 1, & i = p \\ 0, & i \neq p, \end{cases} \tag{2.12}$$

$$\delta_{pi}^{(1)} \equiv h\left[\frac{d}{d\chi}S(p,h)\circ\chi(z)\right]\Big|_{z=z_i} = \begin{cases} 0, & i=p \\ \dfrac{(-1)^{i-p}}{(i-p)}, & i\neq p, \end{cases} \tag{2.13}$$

$$\delta_{pi}^{(2)} \equiv h^2\left[\frac{d^2}{d\chi^2}S(p,h)\circ\chi(z)\right]\Big|_{z=z_i} = \begin{cases} -\dfrac{\pi^2}{3}, & i=p \\ \dfrac{(-2)(-1)^{i-p}}{(i-p)^2}, & i\neq p, \end{cases} \tag{2.14}$$

$$\delta_{pi}^{(3)} \equiv h^3\left[\frac{d^3}{d\chi^3}S(p,h)\circ\chi(z)\right]\Big|_{z=z_i} = \begin{cases} 0, & i=p \\ \dfrac{(-1)^{i-p}}{(i-p)^3}[6-\pi^2(i-p)^2], & i\neq p, \end{cases} \tag{2.15}$$

and

$$\delta_{pi}^{(4)} \equiv h^4\left[\frac{d^4}{d\chi^4}S(p,h)\circ\chi(z)\right]\Big|_{z=z_i} = \begin{cases} \dfrac{\pi^4}{5}, & i=p \\ \dfrac{-4(-1)^{i-p}}{(i-p)^4}[6-\pi^2(i-p)^2], & i\neq p \end{cases} \tag{2.16}$$

which denote the evaluation at the gridpoint z_i of the sinc-map compositions and their derivatives with respect to the map χ.

3 The Forward Problem

Two forward problems of interest are

$$\begin{aligned} \mathcal{L}u(x,t) \equiv \frac{\partial^2 u}{\partial t^2}(x,t) + \frac{\partial^2}{\partial x^2}\left(EI(x)\frac{\partial^2 u}{\partial x^2}(x,t)\right) = f(x,t), \quad 0<x<1 \quad t>0 \\ u(0,t)=u(1,t)=0, \quad t>0 \\ \frac{\partial u}{\partial x}(0,t)=\frac{\partial u}{\partial x}(1,t)=0, \quad t>0 \\ u(x,0)=\frac{\partial u}{\partial t}(x,0)=0, \quad 0\le x\le 1 \end{aligned} \tag{3.1}$$

and

$$\begin{aligned} \mathcal{L}u(x,t) &= f(x,t), \quad 0 < x < 1, \quad t > 0 \\ u(0,t) = \overline{\alpha}(t), &\quad \left(EI\frac{\partial^2 u}{\partial x^2}\right)(1,t) = \overline{\gamma}(t), \quad t > 0 \\ \frac{\partial u}{\partial x}(0,t) = \overline{\beta}(t), &\quad \frac{\partial}{\partial x}\left(EI\frac{\partial^2 u}{\partial x^2}\right)(1,t) = \overline{\delta}(t), \quad t > 0 \\ u(x,0) = \frac{\partial u}{\partial t}(x,0) &= 0, \quad 0 \le x \le 1 \ . \end{aligned} \tag{3.2}$$

Since a thorough derivation of the Sinc-Galerkin method for problems of this type is given in [18], the following discussion contains only that material which is needed for the construction of the associated matrix systems.

To define the Sinc-Galerkin approximation to (3.1), let $S_i(x) \equiv S(i,h_x) \circ \phi(x)$ and $S_j^*(t) \equiv S(j,h_t) \circ \Upsilon(t)$, and take the basis to be $\{S_{ij}\}_{i=-M_x,\cdots,N_x}^{j=-M_t,\cdots,N_t}$ where

$$S_{ij}(x,t) \equiv S_i(x)S_j^*(t).$$

The approximate solution is then defined by way of the tensor product expansion

$$u_{m_x,m_t}(x,t) = \sum_{i=-M_x}^{N_x} \sum_{j=-M_t}^{N_t} u_{ij}S_{ij}(x,t), \qquad \begin{aligned} m_x &= M_x + N_x + 1 \\ m_t &= M_t + N_t + 1. \end{aligned} \tag{3.3}$$

The $m_x \cdot m_t$ unknown coefficients $\{u_{ij}\}$ are determined by orthogonalizing the residual with respect to the set of sinc functions $\{S_pS_q^*\}_{p=-M_x,\cdots,N_x}^{q=-M_t,\cdots,N_t}$. This yields the discrete Galerkin system

$$(\mathcal{L}u_{m_x m_t} - f, S_pS_q^*) = 0 \tag{3.4}$$

for $p = -M_x, \cdots, N_x$ and $q = -M_t, \cdots, N_t$. The inner product $(\cdot,\cdot)$ is taken to be

$$(F,G) = \int_0^\infty \int_0^1 F(x,t)G(x,t)w(x,t)dxdt \tag{3.5}$$

with the weight

$$w(x,t) = w(x)w^*(t) = (\phi'(x))^{-\frac{3}{2}}(\dot{\Upsilon}(t))^{-\frac{1}{2}}. \tag{3.6}$$

The expressions (3.1), (3.4), and (3.5) are combined to form the system

$$\int_0^\infty \int_0^1 \frac{\partial^2}{\partial t^2}(u_{m_x m_t}(x,t)) S_p(x) S_q^*(t) w(x) w^*(t) dx dt$$

$$+ \int_0^\infty \int_0^1 \frac{\partial^2}{\partial x^2}\left(EI(x) \frac{\partial^2}{\partial x^2} u_{m_x,m_t}(x,t)\right) S_p(x) S_q^*(t) w(x) w^*(t) dx dt \qquad (3.7)$$

$$= \int_0^\infty \int_0^1 f(x,t) S_p(x) S_q^*(t) w(x) w^*(t) dx dt$$

for $p = -M_x, \cdots, N_x$ and $q = -M_t, \cdots, N_t$.

In anticipation of the parameter identification problem which motivates this analysis, the term $EI(x)$ in (3.7) is expanded as a linear combination of weighted sinc functions with four Hermite-like algebraic terms added to accommodate the potentially nonzero function and derivative values of EI at $x = 0$ and $x = 1$. Specifically, this parameter basis is taken to be $\{\psi_k\}_{k=-M_x}^{N_x}$ with

$$\psi_k(x) = \begin{cases} b_{-M_x}(x), & k = -M_x \\ b_{-M_x+1}(x), & k = -M_x + 1 \\ v_E(x) S_k(x), & k = -M_x + 2, \cdots, N_x - 2 \\ b_{N_x-1}(x), & k = N_x - 1 \\ b_{N_x}(x), & k = N_x. \end{cases} \qquad (3.8)$$

Here $S_k(x) = S(k, h_x) \circ \phi(x)$ and the basis weight function v_E is

$$v_E(x) = w(x) = [x(1-x)]^{\frac{3}{2}}. \qquad (3.9)$$

The algebraic boundary basis functions are given by

$$b_{-M_x+1}(x) = (1-x)^2[2x+1],$$

$$b_{N_x-1}(x) = x^2[2(1-x)+1],$$

$$b_{-M_x}(x) = x(1-x)^2,$$

and

$$b_{N_x}(x) = -(1-x)x^2.$$

The finite dimensional approximation of EI then takes the form

$$EI_{m_B}(x) = \sum_{k=-M_B}^{N_B} c_k \psi_k(x) \tag{3.10}$$

where the choices $M_E = M_x$ and $N_E = N_x$ are made so as to guarantee a square spatial coefficient matrix. In the forward problem, the coefficients $\{c_k\}_{k=-M_B}^{N_B}$ are known whereas in the corresponding parameter recovery problem, they are unknown and are determined via methods to be discussed in Section 4.

A quick note should be made concerning the choice of parameter basis and the manner of expanding EI_{m_B}. The two derivative-interpolating boundary basis functions are added so that this expansion of EI_{m_B} is the same as that used with cantilever or free boundary conditions. The choice of (3.9) for basis weight is certainly sufficient and proves to be beneficial when incorporating this forward scheme into a numerical method for solving the parameter recovery problem as described in Section 4.

The expansion (3.10) is substituted into (3.7), and integration by parts is used to transfer the derivatives onto the product $S_p w S_q^* w^*$. As detailed in [18], the weight choice (3.6) guarantees that all boundary terms vanish. The resulting integrals are evaluated via Theorem 2.2, or when possible, Theorem 2.1. The requirement

$$|\mathcal{EI}(x)u(x,t)| \leq K x^{\alpha+\frac{3}{2}}(1-x)^{\beta+\frac{3}{2}} t^{\gamma+\frac{1}{2}} t^{-\delta} ,$$

where the "homogeneous" part of EI is

$$\mathcal{EI}(x) = EI(x) - EI(0)b_{-M_x+1}(x) - EI(1)b_{N_x-1}(x) - EI'(0)b_{-M_x}(x) - EI'(1)b_{N_x}(x), \tag{3.11}$$

guarantees the decay needed to truncate the infinite quadrature rule as specified by (2.10). With α, β, γ and δ specified and M_x chosen, the choices

$$h_x = \sqrt{\frac{\pi d}{\alpha M_x}}, \tag{3.12}$$

$$h_t = h_x, \tag{3.13}$$

$$N_x = \left[\!\left[\frac{\alpha}{\beta} M_x + 1 \right]\!\right], \tag{3.14}$$

$$M_t = \left[\!\left[\frac{\alpha}{\gamma} M_x + 1 \right]\!\right], \tag{3.15}$$

and

$$N_t = \left[\left[\frac{\gamma}{\delta} M_t + 1\right]\right] \tag{3.16}$$

for the stepsizes and summation limits balance the asymptotic errors to at least order $\mathcal{O}\left(e^{(-\pi d\alpha M_x)^{\frac{1}{2}}}\right)$. This rate results from the presence of a sinc function in the integral. In the above expressions, $[\cdot]$ denotes the greatest integer function. Note that the $+1$ is unnecessary when $\frac{\alpha}{\beta} M_x$, $\frac{\alpha}{\gamma} M_x$, or $\frac{\gamma}{\delta} M_t$ are integers.

In many time-dependent problems, the solution decays exponentially at infinity; that is, the solution satisfies

$$|\mathcal{EI}(x)u(x,t)| \leq K x^{\alpha+\frac{3}{2}}(1-x)^{\beta+\frac{3}{2}} t^{\gamma+\frac{1}{2}} e^{-\delta t}. \tag{3.17}$$

With this supposition, Lund [11] shows that the condition (3.16) can be replaced by

$$N_t = \left[\left[\frac{1}{h_t} ln\left(\frac{\gamma}{\delta} M_t h_t\right) + 1\right]\right]. \tag{3.18}$$

The selection N_t in (3.18) significantly reduces the size of the discrete system with no loss of accuracy.

Given M_x, N_x, M_t, N_t and $h = h_x = h_t$ as defined above, the discrete system for (3.1) is

$$A(EI)UC_t^T + C_x U A_t^T = G. \tag{3.19}$$

Here

$$C_t \equiv \mathcal{D}\left(\frac{w^*}{\dot{\Upsilon}}\right), \tag{3.20}$$

$$C_x \equiv \mathcal{D}\left(\frac{w}{\phi'}\right), \tag{3.21}$$

and

$$G \equiv \mathcal{D}\left(\frac{w}{\phi'}\right) F \mathcal{D}\left(\frac{w^*}{\dot{\Upsilon}}\right) \tag{3.22}$$

where $\mathcal{D}(\eta)$ denotes the diagonal matrix with entries $\eta(x_{-M_x}), \cdots, \eta(x_{N_x})$. The $m_x \times m_t$ matrices U and F are defined componentwise by

$$[U]_{ij} = u_{ij}$$

and

$$[F]_{ij} = f(x_i, t_j).$$

It should be noted that the ordering of the coefficients u_{ij} in U mimics that used in most standard time-differencing schemes. This is a matter of convenience since the Sinc-Galerkin method is not bound by any specific ordering of the grid.

To simplity notation when specifying the spatial and temporal matrices $A(EI)$ and A_t respectively, let $I^{(\ell)}$, $\ell = 0,1,2,3,4$ denote the matrices whose pi-th entry is $\delta_{pi}^{(\ell)}$ from (2.12) - (2.16). As shown in [13], the $m_t \times m_t$ matrix A_t is given by

$$A_t = \left[\frac{1}{h_t^2} I^{(2)} - \frac{1}{4} I^{(0)}\right] \mathcal{D}((\dot{\Upsilon})^{\frac{1}{2}}). \tag{3.23}$$

The $m_x \times m_x$ matrix $A(EI)$ has the form

$$A(EI) = \left[\Phi^{(2)}\mathcal{D}(\vec{p}_{\Psi^{(2)}}) + 2\Phi^{(3)}\mathcal{D}(\vec{p}_{\Psi^{(1)}}) + \Phi^{(4)}\mathcal{D}(\vec{p}_{\Psi^{(0)}})\right]. \tag{3.24}$$

The notation $\mathcal{D}(\vec{p}_{\Psi^{(\ell)}})$, $\ell = 0,1,2$ denotes the diagonal matrices containing the components of the vectors

$$\vec{p}_{\Psi^{(\ell)}} = \Psi^{(\ell)}\vec{c}, \quad \ell = 0,1,2 \tag{3.25}$$

where $\vec{c} = [c_{-M_x}, \cdots, c_{N_x}]^T$. The matrices $\Phi^{(j)}$, $j = 2,3,4$ and $\Psi^{(\ell)}$, $\ell = 0,1,2$ are defined componentwise by

$$[\Phi^{(j)}]_{pi} = \frac{1}{\phi'(x_i)}(S_p w)^{(j)}(x_i) \tag{3.26}$$

and

$$[\Psi^{(\ell)}]_{ik} = \psi_k^{(\ell)}(x_i). \tag{3.27}$$

with the notation on the right-hand sides of (3.26) and (3.27) indicating the j-th and ℓ-th derivatives, respectively.

To illustrate the dependence of $\Phi^{(j)}$, $j = 2,3,4$ and $\Psi^{(\ell)}$, $\ell = 0,1,2$ on fundamental matrices, the respective expansions are listed below. The diagonal matrices $\mathcal{D}$ and the matrices $I^{(\ell)}$, $\ell = 0,1,2,3,4$ have sizes consistent with the following range of indices i, p, and k ($-M_x \le i \le N_x, -M_x \le p \le N_x, -M_x + 2 \le k \le N_x - 2$). From (3.26) it follows that

$$\Phi^{(2)} = \frac{1}{h_x^2} I^{(2)} \mathcal{D}(w\phi') + \frac{1}{h_x} I^{(1)} \mathcal{D}(2w') + I^{(0)} \mathcal{D}(w''), \tag{3.28}$$

$$\begin{aligned} \Phi^{(3)} &= \frac{1}{h_x^3} I^{(3)} \mathcal{D}\left(w(\phi')^2\right) + \frac{1}{h_x^2} I^{(2)} \mathcal{D}(3w'\phi' + 3w\phi'') \\ &\quad + \frac{1}{h_x} I^{(1)} \mathcal{D}\left(3w'' + 3w'\frac{\phi''}{\phi'} + w\frac{\phi'''}{\phi'}\right) + I^{(0)} \mathcal{D}\left(\frac{w'''}{\phi'}\right) \end{aligned} \tag{3.29}$$

and

$$\begin{aligned} \Phi^{(4)} &= \frac{1}{h_x^4} I^{(4)} \mathcal{D}\left(w(\phi')^3\right) + \frac{1}{h_x^3} I^{(3)} \mathcal{D}\left(4w'(\phi')^2 + 6w\phi'\phi''\right) \\ &\quad + \frac{1}{h_x^2} I^{(2)} \mathcal{D}\left(6w''\phi' + 12w'\phi'' + 4w\phi''' + 3w\frac{(\phi'')^2}{\phi'}\right) \\ &\quad + \frac{1}{h_x} I^{(1)} \mathcal{D}\left(4w''' + 6w''\frac{\phi''}{\phi'} + 4w'\frac{\phi'''}{\phi'} + w\frac{\phi'''}{\phi'}\right) \\ &\quad + I^{(0)} \mathcal{D}\left(\frac{w'''}{\phi'}\right). \end{aligned} \tag{3.30}$$

For $\ell = 0, 1, 2$ the $m_x \times m_x$ matrices in (3.27) are given by

$$\Psi^{(\ell)} = \left[\vec{b}^{(\ell)}_{-M_x} \vdots \vec{b}^{(\ell)}_{-M_x+1} \vdots B^{(\ell)} \vdots \vec{b}^{(\ell)}_{N_x-1} \vdots \vec{b}^{(\ell)}_{N_x}\right] \tag{3.31}$$

where $\vec{b}^{(\ell)}_k = [b^{(\ell)}_k(x_{-M_x}), \cdots, b^{(\ell)}_k(x_{N_x})]^T$ for $k = -M_x, -M_x + 1, N_x - 1$ and N_x. Again, the superscript ℓ indicates the ℓ-th derivative. The $m_x \times (m_x - 4)$ matrices $B^{(\ell)}$ are

$$B^{(0)} = \mathcal{D}(v_E) I^{(0)}, \tag{3.32}$$

$$B^{(1)} = -\frac{1}{h_x} \mathcal{D}(v_E\phi') I^{(1)} + \mathcal{D}(v_E) I^{(0)} \tag{3.33}$$

and

$$B^{(2)} = \frac{1}{h_x^2} \mathcal{D}\left(v_E(\phi')^2\right) I^{(2)} - \frac{1}{h_x} \mathcal{D}(v_E\phi' + 2v_E'\phi') I^{(1)} + \mathcal{D}(v_E'') I^{(0)}. \tag{3.34}$$

The negative signs that appear in the definitions of $B^{(1)}$ and $B^{(2)}$ result from the transposing of $I^{(1)}$. Again, it is noted that in (3.32) - (3.34), the $m_x \times (m_x - 4)$ matrices $I^{(\ell)}, \ell = 0, 1, 2$ have components $\delta^{(\ell)}_{ik}$ as defined in (2.12) - (2.14).

Various methods exist for solving matrix systems of the form (3.19), one of which derives from the generalized Schur decomposition (page 396 of [4]). As guaranteed by the results of Moler and Stewart [15], there exist unitary matrices Q_1, Z_1, Q_2 and Z_2 such that

$$Q_1^* A_x Z_1 = P$$

$$Q_1^* C_x Z_1 = R$$

$$Q_2^* C_t Z_2 = S$$

$$Q_2^* A_t Z_2 = T$$

where P, R, S, and T are upper triangular. If $Y = Z_1^* U Z_2$ and $C = Q_1^* G Q_2$, then (3.19) transforms to

$$PYT^* + RYS^* = C.$$

By comparing the k-th columns, one finds that

$$P \sum_{j=k}^{n} t_{kj} y_j + R \sum_{j=k}^{n} s_{kj} y_j = c_k$$

which yields

$$(t_{kk} P + s_{kk} R) y_k = c_k - P \sum_{j=k+1}^{n} t_{kj} y_j - R \sum_{j=k+1}^{n} s_{kj} y_j \tag{3.35}$$

(for convenience, it is assumed that all matrices are $n \times n$ and indexed from 1 to n). With the assumption that the matrix $(t_{kk} P + s_{kk} R)$ is nonsingular, the solution to (3.35) is easily found by recursively solving triangular systems.

Although this algorithm does require complex algebra, it is both robust and efficient and requires no assumptions concerning the diagonalizability of the component matrices. It should be noted that a "real" version of this algorithm also exists [3]. In this latter algorithm, Q_1, Z_1, Q_2, and Z_2 are orthogonal with P, S quasi-upper triangular and R, T upper triangular.

A Sinc-Galerkin method for the more general problem (3.2) can be developed in a similar manner once a suitable basis has been determined for discretizing the spatial variable. To

this end, define the set of spatial basis function $\{\zeta_i\}_{i=-M_x-4}^{N_x+4}$ by

$$\zeta_i(x) = \begin{cases} B_{-M_x-4}(x), & i = -M_x - 4 \\ B_{-M_x-3}(x), & i = -M_x - 3 \\ B_{-M_x-2}(x), & i = -M_x - 2 \\ B_{-M_x-1}(x), & i = -M_x - 1 \\ v(x)S_i(x), & i = -M_x, \cdots, N_x \\ B_{N_x+1}(x), & i = N_x + 1 \\ B_{N_x+2}(x), & i = N_x + 2 \\ B_{N_x+3}(x), & i = N_x + 3 \\ B_{N_x+4}(x), & i = N_x + 4. \end{cases} \tag{3.36}$$

Here $S_i(x) \equiv S(i, h_x) \circ \phi(x)$ and the basis weight $v(x)$ is taken to be

$$v(x) = [x(1-x)]^3. \tag{3.37}$$

The boundary basis functions are

$$B_{-M_x-1}(x) = (1-x)^4[20x^3 + 10x^2 + 4x + 1],$$

$$B_{N_x+1}(x) = x^4[20(1-x)^3 + 10(1-x)^2 + 4(1-x) + 1],$$

$$B_{-M_x-2}(x) = x(1-x)^4[10x^2 + 4x + 1],$$

$$B_{N_x+2}(x) = -x^4(1-x)[10(1-x)^2 + 4(1-x) + 1],$$

$$B_{-M_x-3}(x) = x^2(1-x)^4\left[2x + \frac{1}{2}\right],$$

$$B_{N_x+3}(x) = x^4(1-x)^2\left[2(1-x) + \frac{1}{2}\right],$$

$$B_{-M_x-4}(x) = \frac{1}{6}x^3(1-x)^4,$$

and

$$B_{N_x+4}(x) = -\frac{1}{6}x^4(1-x)^3.$$

A brief note concerning the choice of spatial basis is in order at this point. First, since $\frac{d^{(\ell)}}{dx^{(\ell)}}[S(i,h_x)\circ\phi(x)]$, $\ell = 1,2,\cdots$, are undefined at $x = 0$ and $x = 1$, some basis modifications must be made when solving problems with nonzero boundary conditions (see also the definition of ψ_k in (3.8)). With the cantilever boundary conditions of (3.2), it is tempting to use fewer algebraic boundary basis functions and the basis weight

$$v(x) = x(1-x)^3$$

but in many problems this results in nonzero boundary terms when integrating by parts. By using the symmetric basis weight $v(x) = [x(1-x)]^3$ and a full complement of algebraic terms, this pitfall can be avoided. Furthermore, the spatial basis $\{\zeta_i\}$ as defined in (3.36) can be used for problems with free boundary conditions, thus providing consistency to the method.

The basis for the problem (3.2) is then taken to be $\{\zeta_i S_j^*\}$ with $S_j^*(t) = S(j,h_t)\circ\Upsilon(t)$, and the approximate solution is defined to be

$$\begin{aligned} u_{m_x m_t}(x,t) \;=\; & \sum_{i=-M_x}^{N_x}\sum_{j=-M_t}^{N_t} u_{ij}\zeta_i(x)S_j^*(t) \\ & + \sum_{j=-M_t}^{N_t} S_j^*(t)\{u_{-M_x-3,j}\zeta_{-M_x-3}(x) + u_{-M_x-4,j}\zeta_{-M_x-4}(x) \\ & \quad + u_{N_x+1,j}\zeta_{N_x+1}(x) + u_{N_x+2,j}\zeta_{N_x+2}(x)\} \\ & + \{\overline{\alpha}(t)\zeta_{-M_x-1}(x) + \overline{\beta}(t)\zeta_{-M_x-2}(x) + \tilde{\gamma}(t)\zeta_{N_x+3}(x) + \tilde{\delta}(t)\zeta_{N_x+4}(x)\} \end{aligned} \tag{3.38}$$

where

$$\tilde{\gamma}(t) = \frac{1}{EI(1)}\overline{\gamma}(t)$$

and

$$\tilde{\delta}(t) = \frac{1}{EI(1)}\overline{\delta}(t) - \frac{EI'(1)}{[EI(1)]^2}\overline{\gamma}(t).$$

The functions $\tilde{\gamma}(t)$ and $\tilde{\delta}(t)$ are well-defined since $EI(x)$ is assumed positive on [0,1]. It should be noted that the approximate solution does satisfy the boundary conditions in (3.2).

The $(m_x+4)\cdot m_t$ unknowns $\{u_{ij}\}$ in (3.38) are determined by orthogonalizing the residual with respect to the sinc functions $\{S_p(x)S_q^*(t)\}_{p=-M_x-2,\cdots,N_x+2}^{q=-M_t,\cdots,N_t}$. This Petrov-Galerkin approach is in contrast to those Galerkin methods in which the residual is orthogonalized

with respect to the basis and is done to take advantage of the exponential accuracy of point evaluation in the quadrature. This yields the discrete system

$$(\mathcal{L}u_{m_x m_t} - f, S_p S_q^*) = 0, \qquad \begin{array}{l} -M_x - 2 \le p \le N_x + 2 \\ -M_t \le q \le N_t \end{array}$$

where $(\cdot,\cdot)$ is defined in (3.5) with $w(x,t) = (\dot{\Upsilon}(t))^{-\frac{1}{2}}$.

Appropriate integration by parts and application of the sinc quadrature rules, as discussed in [18], yields the matrix equation

$$A(EI)UC_t^T + C_x M U A_t^T = G \tag{3.39}$$

where C_t, C_x, and A_t are defined in (3.20), (3.21), and (3.23) respectively, and

$$G = \mathcal{D}\left(\frac{w}{\phi'}\right)\overline{F}\mathcal{D}\left(\frac{w^*}{\dot{\Upsilon}}\right).$$

The $(m_x + 4) \times m_x$ matrices U and $\overline{F}$ are defined componentwise by

$$[U]_{ij} = u_{ij}$$

and

$$[\overline{F}]_{ij} = \overline{f}(x_i, t_j)$$

where

$$\begin{aligned} \overline{f}(x,t) \;\equiv\; & f(x,t) - \mathcal{L}(\overline{\alpha}(t)B_{-M_x-1}(x)) - \mathcal{L}(\overline{\beta}(t)B_{-M_x-2}(x)) \\ & -\mathcal{L}(\tilde{\gamma}(t)B_{N_x+3}(x)) - \mathcal{L}(\tilde{\delta}(t)B_{N_x+4}(x)). \end{aligned}$$

The $(m_x + 4) \times (m_x + 4)$ matrix M has the form

$$M = \left[\begin{array}{c|c|c|c|c} & & & & \\ & 0 & & & \\ & - \; - & & & \\ \hat{b}_{L2} & \hat{b}_{L1} & D_M & \hat{b}_{R1} & \hat{b}_{R2} \\ & - \; - & & & \\ & 0 & & & \end{array}\right]$$

where the $m_x \times m_x$ submatrix D_M and the $(m_x + 4) \times 1$ vectors are given by

$$D_M = \mathcal{D}(v),$$

$$\hat{b}_{L2} = \mathcal{D}(B_{-M_x-4})\vec{1},$$

$$\hat{b}_{L1} = \mathcal{D}(B_{-M_x-3})\vec{1},$$

$$\hat{b}_{R1} = \mathcal{D}(B_{N_x+1})\vec{1}$$

and

$$\hat{b}_{R2} = \mathcal{D}(B_{N_x+2})\vec{1}.$$

Here $\vec{1}$ is simply an $(m_x+4)\times 1$ vector of ones.

The spatial matrix $A(EI)$ can be constructed as follows. Let $\Phi^{(j)}$, $\Psi^{(\ell)}$ and $\vec{p}_{\Psi^{(\ell)}}$ be defined as they were in (3.26), (3.27), and (3.25), respectively (with $\ell = 0,1,2$ and $j = 2,3,4$). Note that in the definitions now, the index ranges are $-M_x \le i \le N_x$, $-M_x-2 \le p \le N_x+2$, and $-M_x-2 \le k \le N_x+2$, and the $(m_x+4)\times 1$ coefficient vector is now $\vec{c} = [c_{-M_x-2}, \cdots, c_{n_x+2}]^T$. Hence $\Phi^{(j)}$, $\Psi^{(\ell)}$ and $\vec{p}_{\Psi^{(\ell)}}$ have the sizes $(m_x+4)\times m_x$, $m_x\times(m_x+4)$ and $m_x\times 1$, respectively.

Furthermore, let $\hat{\Phi}''$ denote the $(m_x+4)\times m_x$ matrix which is defined componentwise by

$$[\hat{\Phi}'']_{pk} = \frac{1}{\phi'(x_k)}(S_p w)''(x_k)$$

and let $\tilde{c} = [c_{-M_x}, \cdots, c_{N_x}]^T$. Finally, for $i = -M_x-4, \cdots, -M_x-1$ and $i = N_x+1, \cdots, N_x+4$, let $\vec{a}_i$ denote the $(m_x+4)\times 1$ vectors

$$\vec{a}_i = \left[\hat{\Phi}''\mathcal{D}(v_E B_i'')\tilde{c} + \mathcal{D}\left(\frac{w}{\phi'}(EI_c B_i'')''\right)\vec{1}\right].$$

Here

$$EI_c(x) \equiv c_{-M_x-1}b_{-M_x-1}(x) + c_{-M_x-2}b_{-M_x-2}(x) + c_{N_x+1}b_{N_x+1}(x) + c_{N_x+2}b_{N_x+2}(x)$$

and $\vec{1}$ is simply the $m_x\times 1$ vector of ones. The $(m_x+4)\times(m_x+4)$ matrix $A(EI)$ is then

$$A(EI) = [\vec{a}_{-M_x-4} \vdots \vec{a}_{-M_x-3} \vdots A_m \vdots \vec{a}_{N_x+1} \vdots \vec{a}_{N_x+2}] \tag{3.40}$$

where the $(m_x+4)\times m_x$ submatrix A_m is given by

$$A_m = \left[\Phi^{(2)}\mathcal{D}(v)\mathcal{D}(\vec{p}_{\Psi^{(2)}}) + 2\Phi^{(3)}\mathcal{D}(v)\mathcal{D}(\vec{p}_{\Psi^{(1)}}) + \Phi^{(4)}\mathcal{D}(v)\mathcal{D}(\vec{p}_{\Psi^{(0)}})\right].$$

It should be noted that the coefficient matrix $A(EI)$ in (3.40) differs from that arising in the fixed boundary problem, (3.24), only in the presence of the diagonal multipliers $\mathcal{D}(v)$

and the addition of border vectors. Hence the method is easily adapted when changing the boundary conditions. Furthermore, the matrices $\Phi^{(j)}$, $\hat{\Phi}''$, and $\Psi^{(\ell)}$ can be expanded in terms of fundamental matrices in a manner similar to that in (3.28) - (3.34), thus simplifying the implementation of the method.

With $A(EI), A_t, C_x, C_t, M$, and G thus specified, the system (3.39) can be solved via the generalized Schur algorithm (3.35).

The final implementation issue for the forward problem (3.2) concerns the choice of decay parameters α, β, γ, and δ. As discussed in [18], the weight choice $w(x,t) = (\dot{\Upsilon}(t))^{-\frac{1}{2}}$ yields the decay condition

$$|\mathcal{EI}(x)\mathcal{U}(x,t)| \leq x^{\alpha+3}(1-x)^{\beta+3}t^{\gamma+\frac{1}{2}}e^{-\delta t} \tag{3.41}$$

where $\mathcal{EI}(x)$ is defined in (3.11) and $\mathcal{U}(x,t)$ is that part of the true solution which is approximated by

$$u_h(x,t) = \sum_{i=-M_x}^{N_x} \sum_{j=-M_t}^{N_t} u_{ij}\zeta_i(x)S_j^*(t)$$

(this can be formally obtained by subtracting all boundary contributions from the true solution $u(x,t)$). With the decay parameters specified and M_x chosen, the remaining stepsizes and summation limits are given by (3.12) - (3.16).

4 The Finite Dimensional Minimization Problem

As noted in the introduction, the minimization problem

$$\min_{EI \in Q} \mathcal{T}_\alpha(EI)$$

where

$$\mathcal{T}_\alpha(EI) = \frac{1}{2}\{\|\mathcal{K}(EI) - d\|^2 + \alpha\|EI\|_Q^2\}$$

is infinite dimensional and thus must be replaced by a sequence of finite dimensional problems before a viable numerical scheme can be developed. Following from (3.10), the approximating admissible parameter sets are taken to be

$$Q_{m_E} = \left\{ EI_{m_E} : EI_{m_E}(x) = \sum_{k=-M_E}^{N_E} c_k\psi_k(x) \right\}, \quad m_E = M_E + N_E + 1$$

with the basis $\{\psi_k\}$ defined in (3.8). The summation limits depend on the boundary conditions with $M_E = M_x, N_E = N_x$ for fixed boundary conditions and $M_E = M_x+2, N_E = N_x+2$ for cantilever boundary conditions. The associated finite dimensional optimization problem can then be formulated as

$$\min_{EI_{m_B} \in Q_{m_B}} \hat{T}_\alpha(EI_{m_B}) \tag{4.1}$$

where

$$\hat{T}_\alpha(EI_{m_B}) = \frac{1}{2}\{\|\hat{K}(EI_{m_B}) - \vec{d}\|^2 + \alpha\|EI_{m_B}\|_Q^2\}. \tag{4.2}$$

Note that in solving the minimization problem (4.1), one is actually solving for the vector $\vec{c} = [c_{-M_B}, \cdots, c_{N_B}]^T \in \mathbb{R}^{m_B}$ which minimizes $\hat{T}_\alpha$.

With n_p and n_q specifying the number of spatial and temporal observation points, respectively, the approximation $\hat{K}(EI_{m_B}) : \mathbb{R}^{m_B} \to \mathbb{R}^{n_p \cdot n_q}$ to $K(EI)$ is obtained by applying a discrete analogue of the observation operator C in (1.6) to $u_{m_x m_t}$ in (3.3) or (3.38). If the set of observation points $\{(x_p, t_q)\}_{p=1,\cdots,n_p}^{q=1,\cdots,n_q}$ can be represented as a tensor product of spatial and temporal points, then $\hat{K}(EI_{m_B})$ has the representation

$$\hat{K}(EI_{m_B}) = C\ \overrightarrow{co(U)} \tag{4.3}$$

where the matrix U solves either (3.19) or (3.39) depending on the boundary conditions. For the fixed boundary problem (3.1), the matrix concatenation $\overrightarrow{co(U)}$ is the vector in $\mathbb{R}^{m_x \cdot m_t}$ which is obtained by successively stacking the columns of the $m_x \times m_t$ matrix U. C is an $(n_p \cdot n_q) \times (m_x \cdot m_t)$ evaluation matrix which can be formulated as follows. Define the $n_p \times m_x$ spatial evaluation matrix E_x to have components

$$[E_x]_{p,i} = S_i(x_p), \quad 1 \le p \le n_p, \quad -M_x \le i \le N_x$$

and let the $n_q \times m_t$ temporal evaluation matrix E_t have the components

$$[E_t]_{q,j} = S_j^*(t_q), \quad 1 \le q \le n_q, \quad -M_t \le j \le N_t.$$

Then

$$C = E_t \otimes E_x.$$

Similar formulations for C and $\overrightarrow{co(U)}$ can be used if the cantilever boundary value problem is being considered. It is noted that if the set of observation points is not rectangular as

described above, then point evaluation can be done directly via (3.3) or (3.38). This latter option is less efficient, however, than that defined in (4.3).

The discrete penalty functional $\|EI_{m_E}\|_Q^2$ is formed by substituting the expansion (3.10) into the definition (1.8). This yields

$$\|EI_{m_E}\|_Q^2 = \int_0^1 [EI''_{m_E}(x)]^2 dx + \epsilon \int_0^1 [EI_{m_E}(x)]^2 dx \approx \vec{c}^T Q \vec{c}$$

where the $m_E \times m_E$ matrix $Q = Q_d + Q_f$ has components

$$[Q_d]_{k\ell} \approx \int_0^1 \psi''_k(x)\psi''_\ell(x)dx, \quad -M_E \leq k, \ell \leq N_E$$

and

$$[Q_f]_{k\ell} \approx \int_0^1 \psi_k(x)\psi_\ell(x)dx, \quad -M_E \leq k, \ell \leq N_E.$$

The matrix entries are approximations in the sense that sinc quadrature rules are used to evaluate many of the integrals.

For the choice of basis functions in (3.8), the matrix Q_d is given by

$$Q_d = \begin{bmatrix} 4 & 6 & \vec{0} & -6 & 2 \\ 6 & 12 & \vec{0} & -12 & 6 \\ \vec{0} & \vec{0} & \hat{Q}_d & \vec{0} & \vec{0} \\ -6 & -12 & \vec{0} & 12 & -6 \\ 2 & 6 & \vec{0} & -6 & 4 \end{bmatrix}.$$

Integration by parts and the application of the sinc quadrature formula (2.11) yields the $(m_E - 4) \times (m_E - 4)$ submatrix

$$\hat{Q}_d = \frac{1}{h_x^4} I^{(4)} - \frac{5}{2}\frac{1}{h_x^2} I^{(2)} + \frac{9}{16} I^{(0)}$$

where again, $I^{(\ell)}, \ell = 0, 2, 4$, denote the matrices whose pi-th entries are $\delta_{pi}^{(\ell)}$ from (2.12), (2.14), and (2.16), respectively. The zeroing of all other quadrature terms is a result of the choice $v_E(x) = (\phi'(x))^{-\frac{3}{2}} = [x(1-x)]^{\frac{3}{2}}$. The notation $\vec{0}$ simply denotes a zero vector of length $m_E - 4$. Because $I^{(4)}$ is positive definite and $I^{(2)}$ is negative definite (see [17]), the

matrix Q_d is nonnegative definite with zero eigenvalues resulting from the configuration of the outer four columns.

Direct integration and sinc quadrature are used to obtain the matrix

$$Q_f = \varepsilon \begin{bmatrix} \frac{1}{105} & \frac{11}{210} & \vec{q}_{\ell 2}^{\,T} & \frac{13}{420} & \frac{-1}{140} \\ \frac{11}{210} & \frac{13}{35} & \vec{q}_{\ell 1}^{\,T} & \frac{9}{70} & \frac{13}{420} \\ \vec{q}_{\ell 2} & \vec{q}_{\ell 1} & \hat{Q}_f & \vec{q}_{r1} & \vec{q}_{r2} \\ \frac{13}{420} & \frac{9}{70} & \vec{q}_{r1}^{\,T} & \frac{13}{35} & \frac{11}{120} \\ \frac{-1}{140} & \frac{13}{420} & \vec{q}_{r2}^{\,T} & \frac{11}{120} & \frac{1}{105} \end{bmatrix}$$

Here

$$\hat{Q}_f = h_x \mathcal{D}(x^3(1-x)^3)$$

where $\mathcal{D}(\eta)$ denotes the diagonal matrix with entries $\eta(x_{-M_B+2}), \cdots, \eta(x_{N_B-2})$. Recall that the sinc gridpoints are defined in (2.7). The vectors $\vec{q}_{\ell 1}, \vec{q}_{\ell 2}, \vec{q}_{r1}$ and $\vec{q}_{r2}$ have components

$$[\vec{q}_{\ell 1}]_k = h_x x_k (1-x_k)^3 [2x_k + 1],$$

$$[\vec{q}_{\ell 2}]_k = h_x (1-x_k) x_k^3 [2(1-x_k) + 1],$$

$$[\vec{q}_{r1}]_k = h_x x_k^2 (1-x_k)^3,$$

and

$$[\vec{q}_{r2}]_k = -h_x (1-x_k)^2 x_k^3$$

for $k = -M_E + 2, \cdots, N_E - 2$. The matrix Q_f is strictly positive definite.

Although the matrix Q is full, it is very efficient to construct since the Toeplitz matrices $I^{(0)}, I^{(2)}$ and $I^{(4)}$ are also needed in the forward solver. For $\varepsilon > 0, Q$ is symmetric and positive definite and hence has a Cholesky decomposition $Q = R^T R$ where R is upper triangular. It then follows that the penalty term $\|EI_{m_B}\|_Q^2$ yields the quadratic form

$$\vec{c}^{\,T} R^T R \vec{c} = \|R\vec{c}\|^2 \tag{4.4}$$

where $\|\cdot\|$ denotes the Euclidean norm. This representation for the penalty functional is particularly useful both when implementing a scheme to solve the minimization problem and when plotting the L-curve to determine a suitable regularization parameter α (see [6]).

To highlight the dependence of the functional $\hat{T}_\alpha$ in (4.2) on the unknown vector $\vec{c} = [c_{-M_B}, \cdots, c_{N_B}]^T$, let

$$K(\vec{c}) \equiv \hat{K}(EI_{m_B}) = C\ \overrightarrow{co}(U\ (\vec{c}))$$

where $U(\vec{c})$ solves either (3.19) or (3.39) for a given expansion $EI_{m_B}(x) = \sum_{k=-M_B}^{N_B} c_k \psi_k(x)$. Noting (4.4), the optimization problem (4.1) can be replaced by

$$\min_{\vec{c} \in R^{m_B}} T_\alpha(\vec{c}) \tag{4.5}$$

where

$$T_\alpha(\vec{c}) = \frac{1}{2}\{\|K(\vec{c}) - \vec{d}\|^2 + \alpha\|R\vec{c}\|^2\}. \tag{4.6}$$

To obtain a minimizer for the nonlinear functional $T_\alpha(\vec{c})$, a quasi-Newton/trust region iteration [2]

$$\vec{c}_{k+1} = \vec{c}_k + \vec{s}_k$$

is used. Here $\vec{s}_k$ solves the quadratic programming problem

$$\min_{\vec{s} \in R^{m_B}} \frac{1}{2}\left\{\|K(\vec{c}_k) + K'(\vec{c}_k)\vec{s} - \vec{d}\|^2 + \alpha\|R(\vec{c}_k + \vec{s})\|^2\right\}$$

subject to $\|\vec{s}\| \leq \delta_k$ with $K'(\vec{c}_k)$ denoting the Jacobian of K at $\vec{c}_k$. The trust region radius δ_k is chosen so that $T_\alpha(\vec{c})$ has sufficient decrease at each iteration to guarantee convergence to a local minimizer of T_α (for further details about the theory and implementation of the trust region algorithm, see [2] or [8]). An important numerical issue in the implementation of the trust region scheme is the formulation of the derivative of the operator K. Here the derivative, or Jacobian, is an $(n_p \cdot n_q) \times m_E$ matrix whose ν-th column is given by

$$[K'(\vec{c})]_\nu = \lim_{\mathcal{T} \to 0} \frac{1}{\mathcal{T}}[K(\vec{c} + \mathcal{T}\hat{e}_\nu) - K(\vec{c})]$$

where the standard unit vector $\hat{e}_\nu$ has components

$$[\hat{e}_\nu]_k = \delta_{\nu k} = \begin{cases} 1 & \text{if } k = \nu, \quad -M_E \leq k \leq N_E \\ 0 & \text{otherwise.} \end{cases}$$

In the examples of the next section, the Jacobians were calculated with a standard forward difference scheme. This scheme is easy to implement and accurate enough for the purposes of the method. If further efficiency is desired, a directional derivative scheme such as that described in [12] can be used.

5 Implementation and Numerical Examples

The four examples reported in this section were selected from a large collection of problems to which the Sinc-Galerkin method was applied. The results are representative of those obtained for other problems.

The first example demonstrates the application of the Sinc-Galerkin method to a model problem with fixed boundary conditions in which the state solution was sampled directly; that is, no external noise was added to the data. To demonstrate the feasibility of the method for problems with noisy data, the same problem is revisited in Example 5.2 but with pseudo-random white noise added to the data. In the third example, the parameter to be recovered is the shifted Gaussian function that was discussed for second-order examples in [12] and [19]. Again, pseudo-random white noise is added to the data. The final example demonstrates the application of the method to a problem with cantilever boundary conditions as modeled by (1.2). Hence in this example, the parameter EI appears both in the spatial operator and in the boundary conditions.

In all examples, $d = \frac{\pi}{2}$ (see (2.4) and (2.6)). The errors for the method are reported on the set of uniform gridpoints

$$\begin{aligned} U &= \{z_0, z_1, \cdots, z_{100}\} \\ z_k &= k\ell, \quad k = 0, 1, \cdots, 100 \end{aligned} \tag{5.1}$$

with stepsize $\ell = \frac{1}{100}$. With EI and EI_{m_B} denoting the true and approximate parameters respectively, the errors are reported as

$$\|E_U(\ell)\| = \max_{0 \le k \le 100} |EI(z_k) - EI_{m_B}(z_k)|. \tag{5.2}$$

The error results are tabulated in the form $.aaa - \gamma$ which represents $.aaa \times 10^{-\gamma}$ and all problems were run with sixteen place accuracy on a Vax 8550.

A very important practical consideration is the choice of the regularization parameter α for a given (error-contaminated) data set. If the error in the data is discrete and random, then under certain conditions the method of Generalized Cross Validation (GCV) can be used to determine a suitable value of α [25]. A second method for determining the regularization

parameter is to plot the norm of the penalty functional, $\|R\vec{c}_\alpha\|$, versus the norm of the residual, $\|K(\vec{c}_\alpha) - \vec{d}\,\|$ (see [6] or [14]). Here $\vec{c}_\alpha$ denotes the solution to (4.5). In this way, one can qualitatively get an idea of the compromise between the minimization of these two quantities. The scheme for determining the "optimal" regularization parameter consists of finding those values of α such that $(\|K(\vec{c}_\alpha) - \vec{d}\,\|, \|R\vec{c}_\alpha\|)$ lies in the "corner" of the resulting curve, known as the L-curve. The use of this technique for determining suitable choices for the regularization parameter is demonstrated in the examples.

In all four examples, the data was sampled on a regular grid $\{(x_p, t_q)\} \subset (0,1) \times (0,2]$. Nineteen equally spaced points $x_p = p\Delta x, \Delta x = .05$, were taken in space and four equally spaced temporal points $t_q = q\Delta t, \Delta t = .5$, were taken for a total of $n = 76$ data points. In all examples, the $m_E \times 1$ initial vector $\vec{c}_0 = [.5, .5, .5, \cdots, .5, .5, .5]^T$ was used.

Finally, it should be noted that in the examples, the symbol α is used to denote both the regularization parameter and the sinc decay parameter. The use of this symbol for both quantities is well established in the literature and is thus difficult to avoid in this setting. It should be obvious from the context however, which quantity is being discussed and there should be no ambiguity resulting from the dual use of this symbol.

Example 5.1.

$$\frac{\partial^2 u}{\partial t^2} + \frac{\partial^2}{\partial x^2}\left(EI(x)\frac{\partial^2 u}{\partial x^2}\right) = f(x,t), \quad t > 0 \quad 0 < x < 1$$

$$u(0,t) = u(1,t) = 0, \quad t > 0$$

$$\frac{\partial u}{\partial x}(0,t) = \frac{\partial u}{\partial x}(1,t) = 0, \quad t > 0$$

$$u(x,0) = \frac{\partial u}{\partial t}(x,0) = 0, \quad 0 \le x \le 1$$

The forcing function $f(x,t)$ is consistent with the true stiffness parameter $EI(x) = 1 + \sin(\pi x)$ and the state solution $u(x,t) = x(1-x)\sin(4\pi x)t^2 e^{-t}$. For these functions, the choices $\alpha = \beta = \gamma = \frac{3}{2}$ and $\delta = 1$ satisfy the decay condition (3.17). No noise was added so the data consisted of direct measurements of the state solution. For varying values of the regularization parameter α, the L-curve is plotted in Figure 3. Note that the value $\alpha = 10^{-8}$ yields a point $(\|K(\vec{c}_\alpha) - \vec{d}\,\|, \|R\vec{c}_\alpha\|)$ in the "corner" of the curve. The uniform errors for $\alpha = 10^{-8}$ are reported in Table 1 with the first four columns indicating the index limits

for the expansion of the state variable and the fifth column indicating the number of basis functions used in the expansion of EI_{m_E}. The convergence of the method is demonstrated both by the results in the last column of Table 1 and by Figure 4 which shows the true and approximate stiffness parameters with $\alpha = 10^{-8}$.

M_x	N_x	M_t	N_t	m_E	$\|EI_U(\ell)\|$
8	8	8	4	17	$.1869 - 0$
16	16	16	6	33	$.2482 - 1$
24	24	24	7	49	$.1463 - 2$

Table 1. Errors on the Uniform Grid U with $\alpha = 10^{-8}$ in Example 5.1.

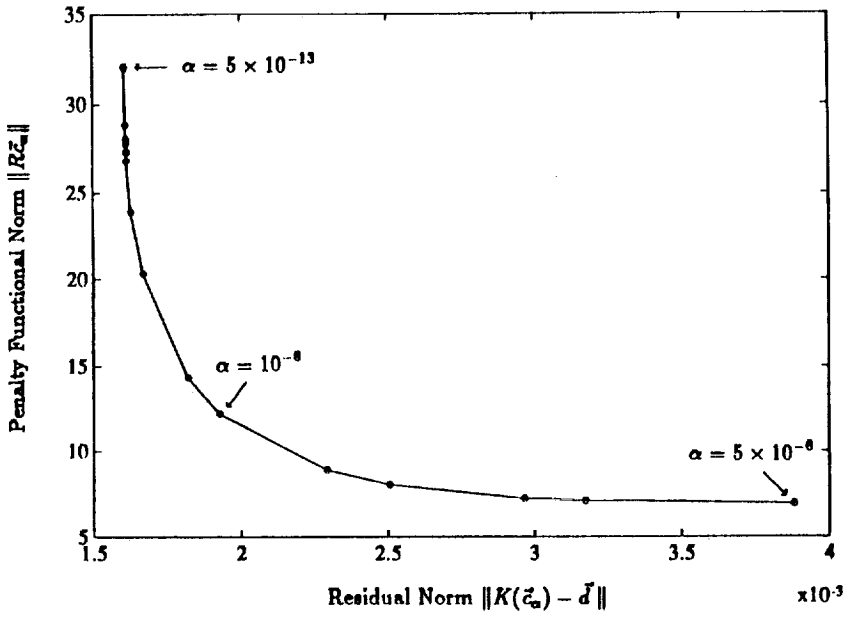

Figure 3. The Tikhonov L-Curve for Example 5.1.

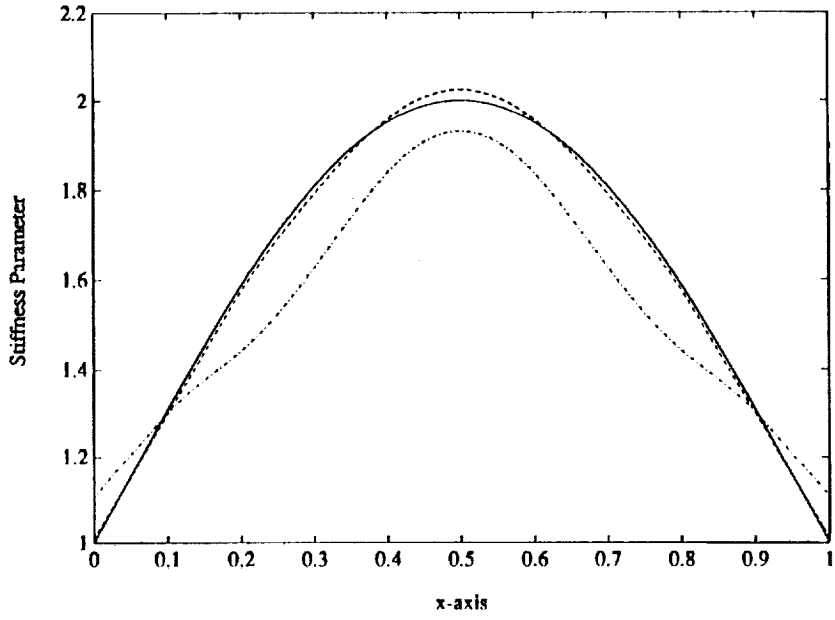

Figure 4. True and Approximate Stiffness Parameters for Example 5.1 with $\alpha = 10^{-8}$ $- \cdot -$ $(m_E = 17)$, $- - -$ $(m_E = 33)$, $\cdots$ $(m_E = 49)$, ——— (True).

Example 5.2.

In this example, the true parameter and state solution are the same as those in Example 5.1, and hence $EI(x) = 1 + \sin(\pi x)$ and $u(x,t) = x(1-x)\sin(4\pi x)t^2e^{-t}$. To the data however, we added a pseudo-random noise vector ϵ from a Gaussian distribution with mean 0 and standard deviation σ chosen so that the noise-to-signal ratio $\sigma/\|\vec{d}\| = .01$; that is, noise $= 1\%$ of the signal. The L-curve is plotted in Figure 5. Note that the values $\alpha = 10^{-5}$ and $\alpha = 5 \times 10^{-6}$ yield points $(\|K(\vec{c}_\alpha) - \vec{d}\|,\ \|R\vec{c}_\alpha\|)$ in the "corner" of the curve. For $m_E = 33$, the uniform errors obtained with $\alpha = 10^{-3}, \alpha = 10^{-5}$ and $\alpha = 10^{-10}$ are given in Table 2. Corresponding plots of the true and approximate stiffness parameters are shown in Figure 6. Note that the "corner" value $\alpha = 10^{-5}$ provides a very good choice for the regularization parameter whereas $\alpha = 10^{-10}$ is not large enough to damp out the error contributions due

to the smaller singular values. Finally, the choice $\alpha = 10^{-3}$ causes too much smoothing and information about the parameter is lost. The results from this example demonstrate the viability of the method for problems with noisy data.

	$\alpha = 10^{-3}$	$\alpha = 10^{-5}$	$\alpha = 10^{-10}$
$\|EI_U(\ell)\|$	$.8503 - 0$	$.2228 - 1$	$.3840 - 1$

Table 2. Errors on the Uniform Grid U with $m_E = 33$ in Example 5.1.

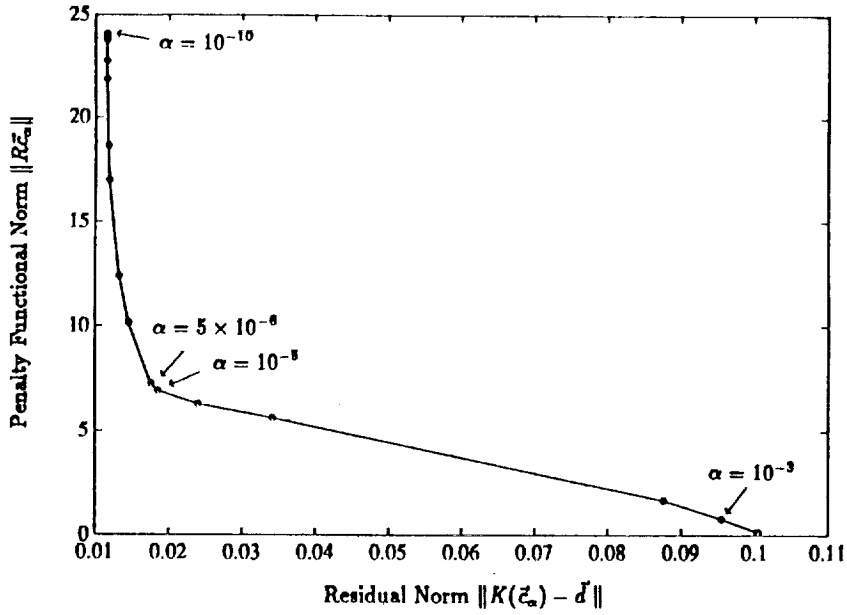

Figure 5. The Tikhonov L-Curve for Example 5.2.

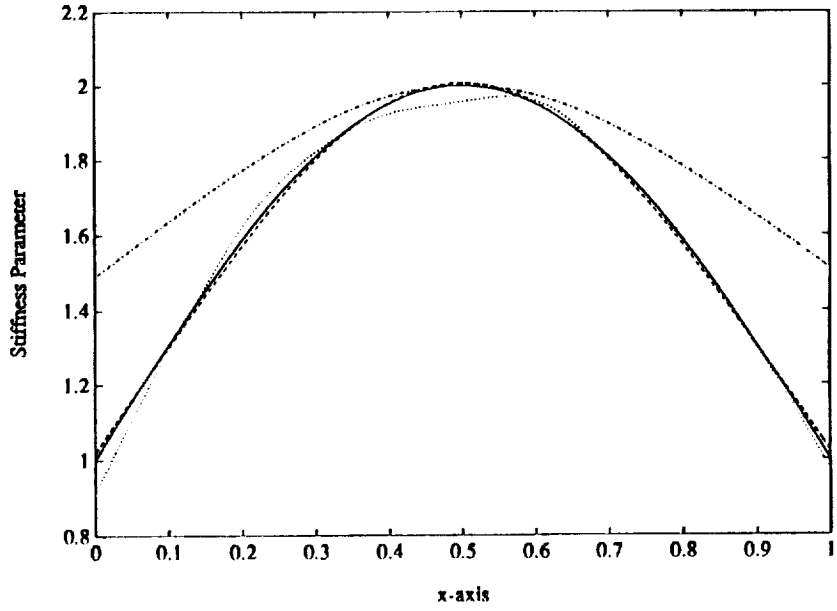

Figure 6. True and Approximate Stiffness Parameters for Example 5.2 with $m_E = 33$
$- \cdot -$ $(\alpha = 10^{-3})$, $- - -$ $(\alpha = 10^{-5})$, $\cdots$ $(\alpha = 10^{-10})$, ——— (True).

Example 5.3.

$$\frac{\partial^2 u}{\partial t^2} + \frac{\partial^2}{\partial x^2}\left(EI(x)\frac{\partial^2 u}{\partial x^2}\right) = f(x,t), \quad t > 0 \quad 0 < x < 1$$
$$u(0,t) = u(1,t) = 0, \quad t > 0$$
$$\frac{\partial u}{\partial x}(0,t) = \frac{\partial u}{\partial x}(1,t) = 0, \quad t > 0$$
$$u(x,0) = \frac{\partial u}{\partial t}(x,0) = 0, \quad 0 \le x \le 1$$

In this example the stiffness parameter to be recovered is the shifted Gaussian function $EI(x) = 1 + \frac{1}{4}e^{-40(x-\frac{1}{3})^2}$. The state solution $u(x,t) = \sin^3(\pi x)t^2e^{-t}$ yields the decay parameters $\alpha = \beta = \gamma = \frac{3}{2}$ and $\delta = 1$ as dictated by (3.17). Pseudo-random noise is again added to the data in the manner described in the last example. As seen in Figure 7, the Tikhonov parameter values $\alpha = 10^{-6}$ through $\alpha = 5 \times 10^{-8}$ yield points $(\|K(\vec{c}_\alpha) - \vec{d}\,\|, \|R\vec{c}_\alpha\|)$ in the "corner" of the L-curve. For the "corner" value $\alpha = 10^{-7}$, numerical results with

$m_E = 17, m_E = 33$ and $m_E = 49$ are reported in Table 3 and Figure 8. In spite of the noise in the data, both sets of results demonstrate that the method converges as the number of basis functions is increased.

M_x	N_x	M_t	N_t	m_E	$\|EI_U(\ell)\|$
8	8	8	4	17	$.1811 - 0$
16	16	16	6	33	$.4191 - 1$
24	24	24	7	49	$.1058 - 1$

Table 3. Errors on the Uniform Grid U with $\alpha = 10^{-7}$ in Example 5.3.

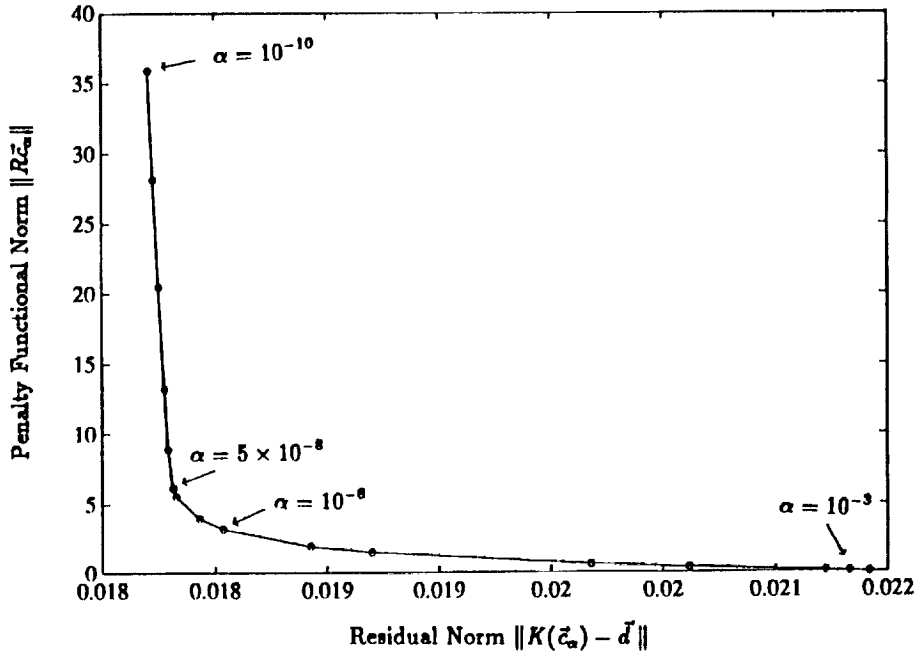

Figure 7. The Tikhonov L-Curve for Example 5.3.

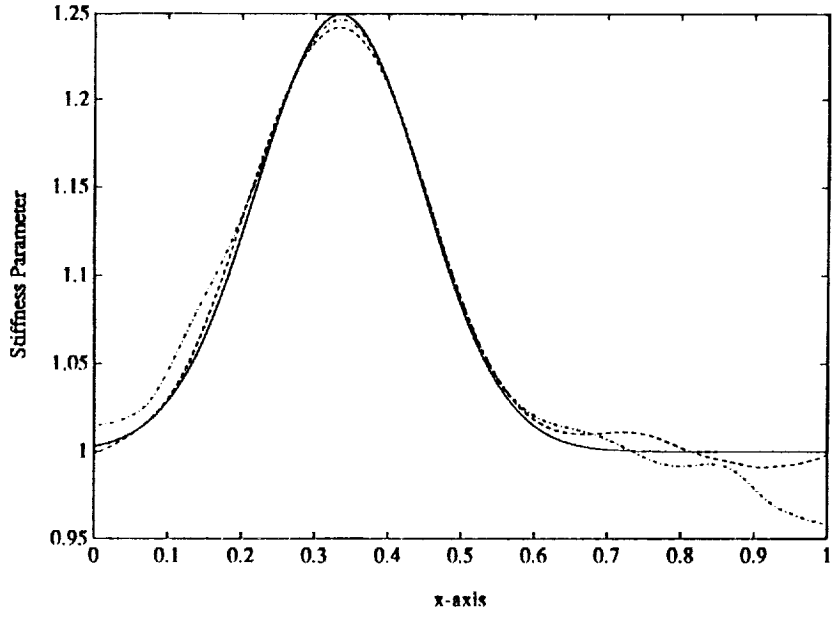

Figure 8. True and Approximate Stiffness Parameters for Example 5.3 with $\alpha = 10^{-7}$
$- \cdot -$ $(m_E = 33)$, $- - -$ $(m_E = 49)$, ——— (True).

Example 5.4.

$$\frac{\partial^2 u}{\partial t^2} + \frac{\partial^2}{\partial x^2}\left(EI(x)\frac{\partial^2 u}{\partial x^2}\right) = f(x,t), \quad t > 0 \quad 0 < x < 1$$

$$u(0,t) = 0, \quad \left(EI\frac{\partial^2 u}{\partial x^2}\right)(1,t) = 0, \quad t > 0$$

$$\frac{\partial u}{\partial x}(0,t) = t^2 e^{-t}, \quad \frac{\partial}{\partial x}\left(EI\frac{\partial^2 u}{\partial x^2}\right)(1,t) = 8\pi^3 t^2 e^{-t}, \quad t > 0$$

$$u(x,0) = \frac{\partial u}{\partial t}(x,0) = 0, \quad 0 \le x \le 1.$$

This example demonstrates the Sinc-Galerkin method for a problem with cantilever boundary conditions and hence the stiffness parameter appears both in the spatial operator and in the boundary conditions themselves. The true stiffness parameter is $EI(x) = 1 + \sin(\pi x)$ and the state solution is $u(x,t) = \sin^3(\pi x)t^2 e^{-t}$. For these functions, the choices $\alpha = \beta = 1, \gamma = \frac{3}{2}$ and $\delta = 1$ satisfy the decay condition (3.41). No noise was added so the data consisted of direct measurements of the state solution. Since the L-curve was very similar to that of

Example 5.1, the regularization parameter was taken to be $\alpha = 10^{-8}$. The uniform errors for this choice are reported in Table 4 and the true and approximate parameters are shown in Figure 9. When comparing Tables 4 and 1, it is noted that the index limits differ as a result of the choice $\alpha = \beta = 1$ for the decay parameters. The smaller values of α and β also indicate why the errors here are slightly larger than those in Example 5.1. Finally, because $M_E = M_x + 2$ and $N_E = N_x + 2$ for these boundary conditions, the number of basis functions, m_E, used in the expansion of EI_{m_E} also differs from the number used in Example 5.1 where $M_E = M_x$ and $N_E = N_x$. Both the table and the figure demonstrate the convergence of the method for problems with cantilever boundary conditions.

M_x	N_x	M_t	N_t	m_E	$\|EI_U(\ell)\|$
8	8	6	3	21	$.1589 - 0$
16	16	11	4	37	$.2589 - 1$
24	24	16	6	53	$.1334 - 1$

Table 4. Errors on the Uniform Grid U with $\alpha = 10^{-8}$ in Example 5.4.

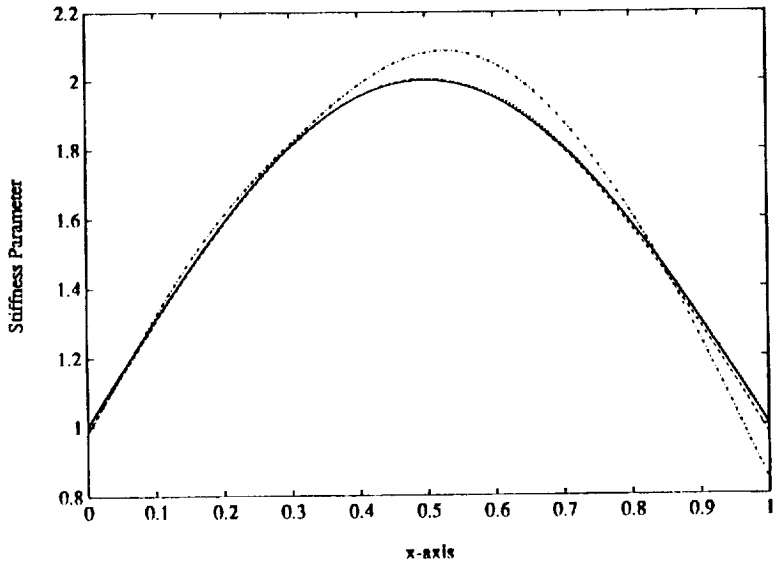

Figure 9. True and Approximate Stiffness Parameters for Example 5.4 with $\alpha = 10^{-8}$
$- \cdot -$ $(m_E = 21)$, $- - -$ $(m_E = 37)$, $\cdots$ $(m_E = 53)$, ——— (True).

References

[1] E.A. Coddington and N. Levinson, *Theory of Ordinary Differential Equations*, McGraw-Hill, New York, 1955.

[2] J.E. Dennis and R.B. Schnabel, *Numerical Methods for Unconstrained Optimization and Nonlinear Equations*, Prentice-Hall, Englewood Cliffs, NJ, 1983.

[3] G.H. Golub, S. Nash and C. VanLoan, "A Hessenberg-Schur Method for the Problem $AX + XB = C$," *IEEE Trans. Automat. Control*, 24, 909-913 (1979).

[4] G.H. Golub and C. VanLoan, *Matrix Computations*, 2nd ed., Johns Hopkins University Press, Baltimore, 1989.

[5] R. Guenther and J. Lee, *Partial Differential Equations of Mathematical Physics and Integral Equations*, Prentice-Hall, Englewood Cliffs, NJ, 1988.

[6] P.C. Hansen, "Analysis of Discrete Ill-Posed Problems by Means of the L-curve," submitted to *SIAM Rev.*

[7] K. Jonca, "Numerical Solution of a Nonlinear Fredholm Integral Equation of the First Kind," PhD Dissertation, Montana State University, 1988.

[8] K. Jonca and C.R. Vogel, "Numerical Solution to the Magnetic Relief Problem," in *Transport Theory, Invariant Imbedding, and Integral Equations (Lecture Notes in Pure and Applied Mathematics)* ed P Nelson *et al*, Marcel Dekker, New York, 379-391 (1989).

[9] K. Kunisch and E. Graif, "Parameter Estimation for the Euler-Bernoulli Beam," *Mat. Aplicada e Computational*, 4, 95-124 (1985).

[10] W. Leighton and Z. Nehari, "On the Oscillation of Solutions of Self-Adjoint Linear Differential Equations of the Fourth Order," *Trans. Am. Math. Soc.*, 89, 325-377 (1968).

[11] J. Lund, "Symmetrization of the Sinc-Galerkin Method for Boundary Value Problems," *Math. Comp.*, 47, 571-588 (1986).

[12] J. Lund and C.R. Vogel, "A Fully-Galerkin Method for the Solution of Inverse Problems in Parabolic Partial Differential Equations," *Inv. Prob.*, 6, 205-217 (1990).

[13] K.M. McArthur, K.L. Bowers and J. Lund, "Numerical Implementation of the Sinc-Galerkin Method for Second-Order Hyperbolic Equations," *Numer. Methods Partial Diff. Equations*, 3, 169-185 (1987).

[14] K. Miller, "Least Squares Methods for Ill-Posed Problems with a Prescribed Bound," *SIAM J. Math. Anal.*, 1, 52-74 (1970).

[15] C.B. Moler and G.W. Stewart, "An Algorithm for Generalized Matrix Eigenvalue Problems," *SIAM J. Numer. Anal.*, 10, 241-256 (1973).

[16] T.I. Seidman and C.R. Vogel, "Well-Posedness and Convergence of Some Regularization Methods for Nonlinear Ill-Posed Problems," *Inv. Prob.*, 5, 227-238 (1989).

[17] R.C. Smith, G.A. Bogar, K.L. Bowers and J. Lund, "The Sinc-Galerkin Method for Fourth-Order Differential Equations," to appear in *SIAM J. Numer. Anal.*

[18] R.C. Smith, K.L. Bowers and J. Lund, "A Fully Sinc-Galerkin Method for Euler-Bernoulli Beam Models," submitted to *Numer. Methods Partial Diff. Equations.*

[19] R.C. Smith and K.L. Bowers, "A Fully Sinc-Galerkin Method for Parameter Estimation in Parabolic Problems," to be submitted to *Inv. Prob.*

[20] I. Stakgold, *Green's Functions and Boundary Value Problems*, Wiley, New York, 1979.

[21] F. Stenger, "Approximations Via Whittaker's Cardinal Function," *J. Approx. Theory*, 17, 222-240 (1976).

[22] F. Stenger, "A Sinc-Galerkin Method of Solution of Boundary Value Problems," *Math. Comp.*, 33, 85-109 (1979).

[23] F. Stenger, "Numerical Methods Based on Whittaker Cardinal, or Sinc Functions," *SIAM Rev.*, 23, 165-224 (1981).

[24] A.N. Tikhonov and V.Y. Arsenin, *Solutions of Ill-Posed Problems*, Wiley, New York, 1977.

[25] G. Wahba, "Practical Approximate Solutions to Linear Operator Equations when the Data are Noisy," *SIAM J. Numer. Anal.*, 14, 651-667 (1977).

NASA
National Aeronautics and Space Administration

Report Documentation Page

1. Report No.	2. Government Accession No.	3. Recipient's Catalog No.
NASA CR-187516 ICASE Report No. 91-14		

4. Title and Subtitle

NUMERICAL RECOVERY OF MATERIAL PARAMETERS IN EULER-BERNOULLI BEAM MODELS

5. Report Date

February 1991

6. Performing Organization Code

7. Author(s)

R.C. Smith
K.L. Bowers
C.R. Vogel

8. Performing Organization Report No.

91-14

10. Work Unit No.

505-90-52-01

9. Performing Organization Name and Address

Institute for Computer Applications in Science and Engineering
Mail Stop 132C, NASA Langley Research Center
Hampton, VA 23665-5225

11. Contract or Grant No.

NAS1-18605

13. Type of Report and Period Covered

Contractor Report

12. Sponsoring Agency Name and Address

National Aeronautics and Space Administration
Langley Research Center
Hampton, VA 23665-5225

14. Sponsoring Agency Code

15. Supplementary Notes

Langley Technical Monitor:
Michael F. Card

Submitted to Journal of Mathematical Systems and Control

Final Report

16. Abstract

A fully Sinc-Galerkin method for recovering the spatially varying stiffness parameter in fourth-order time-dependent problems with fixed and cantilever boundary conditions is presented. The forward problems are discretized with a sinc basis in both the spatial and temporal domains. This yields an approximate solution which converges exponentially and is valid on the infinite time interval. When the forward methods are applied to parameter recovery problems, the resulting inverse problems are ill-posed. Tikhonov regularization is applied and the resulting minimization problems are solved via a quasi-Newton/trust region algorithm. The L-curve method is used to determine an appropriate value of the regularization parameter. Numerical results which highlight the method are given for problems with both fixed and cantilever boundary conditions.

17. Key Words (Suggested by Author(s))	18. Distribution Statement
Sinc-Galerkin method, numerical estimation of stiffness parameters	64 - Numerical Analysis Unclassified - Unlimited

19. Security Classif. (of this report)	20. Security Classif. (of this page)	21. No. of pages	22. Price
Unclassified	Unclassified	40	A03

NASA-Langley, 1991